Research Article   **Open Access**

Calcified Granulomatous Lung Lesions Contain Abundant *Mycobacterium tuberculosis* Components

Tadatsune Iida[1], Keisuke Uchida[1], Nilufar Lokman[1], Asuka Furukawa[1], Yoshimi Suzuki[1], Toshio Kumasaka[2], Tamiko Takemura[2], Hiroshi Kawachi[1], Takumi Akashi[3] and Yoshinobu Eishi[1,3]

[1]Department of Human Pathology, Tokyo Medical and Dental University Graduate School, Tokyo, Japan
[2]Department of Pathology, Japanese Red Cross Medical Center, Tokyo, Japan
[3]Division of Surgical Pathology, Tokyo Medical and Dental University Hospital, Tokyo, Japan

Abstract

Mycobacterium tuberculosis can survive for a long time in the body of a healthy host, causing no symptoms after primary infection. Years or decades later, M. tuberculosis can be reactivated in some carriers, leading to symptoms of post-primary tuberculosis. During the asymptomatic period, *M. tuberculosis* is believed to survive in old foci of infection, yet these foci are uniformly negative by culture and acid-fast staining, which are conventional methods to detect mycobacteria. The precise location and amount of *M. tuberculosis* in these foci, therefore, are not well understood. Here we report that granulomatous lesions with calcification, a well-known characteristic of old tubercles, contained considerable amounts of *M. tuberculosis* genomes and cell wall components. These calcified lesions exhibited little inflammation but all were positive for *M. tuberculosis* by real-time polymerase chain reaction and by immunohistochemistry with a novel monoclonal antibody against lipoarabinomannan, a cell wall component of mycobacteria. We found many lipoarabinomannan-containing granules in the necrotic areas of the lesions that were negative by Ziehl-Neelsen staining but included some bacillus-like structures. The risk of reactivation of latent tuberculosis from these calcified granulomatous lung lesions should be considered.

Introduction

Improved methods to detect and manage latent tuberculosis, such as new diagnostics, drugs, and vaccines, are required to achieve the goal of the World Health Organization to eradicate tuberculosis [1]. At present, the diagnosis of latent tuberculosis is based mainly on immunologic findings, but bacterial carriers cannot be distinguished from non-carriers whose infection has been cured [2]. To efficiently treat latent tuberculosis, a more direct method of determining bacterial carriers is needed. To that end, it is essential to know where and how long-term survival of *Mycobacterium tuberculosis* occurs inside an immunocompetent host's body.

M. tuberculosis is thought to survive for years in old foci of infection, which are fibrous and often calcified lesions [3]. The amounts and precise locations of *M. tuberculosis* in these old lesions, however, have not been well understood [4]. Old lesions, sometimes resected for suspicion of cancer, are uniformly negative for both culture and acid-fast staining, which are current methods used to identify the organism [5].

There are at least two explanations for why these lesions are negative by these testing methods. One is that the lesions seldom contain bacteria or contain only a few bacteria that cannot be detected by these tests. The proliferation ability of *M. tuberculosis* in a latent state might be lower than that in an active state [6], which would make them difficult to culture and detect on thin histologic sections. Another possible explanation for the negative results in these tests is that the tests are not sensitive enough to detect the bacteria. In addition to its low proliferation rate, *M. tuberculosis* loses acid-fastness under

certain experimental conditions, including environmental stress and the absence of a gene related to the synthesis of cell wall components [7-9]. Thus, it is possible that certain amounts of *M. tuberculosis* that have lost acid-fastness are present on the histologic sections of the old lesions, but cannot be detected by acid-fast staining.

To investigate which, if either, of these possibilities accounts for the failed detection of *M. tuberculosis* in old foci by conventional tests, we quantified bacterial genomes and localized their cell wall components in these lesions. We performed quantitative polymerase chain reaction (PCR) for *M. tuberculosis*, which is considered a highly sensitive and specific technique for the detection of *M. tuberculosis* in formalin-fixed and paraffin-embedded (FFPE) tissues [10]. We also performed immunohistochemistry using a novel monoclonal antibody (mAb) against lipoarabinomannan (LAM), which is a cell wall component of mycobacteria [11], to localize *M. tuberculosis* that could not be detected by acid-fast staining.

Materials and Methods

Tissue specimens

FFPE lung tissue specimens that were obtained by surgical resection and contained caseous granulomas/granulomatous lesions (we use the term "granulomatous lesions" because these lesions included

*Corresponding author: Yoshinobu Eishi, Department of Human pathology, Division of Surgical Pathology, Tokyo Medical and Dental University, 1-5-45, Yushima, Bunkyo-ku, Tokyo, 113-8510, Japan, Tel: +81-3-5803-5177; Fax: +81-3-5803-0123; E-mail: eishi.path@tmd.ac.jp

those in which no epithelioid cell layers were observed around the necrotic areas) were collected from the archives of the Japan Red Cross Medical Center (Tokyo, Japan) and the hospital of Tokyo Medical and Dental University (Tokyo, Japan). Specimens containing the largest granulomatous lesion in each patient were selected, and the largest lesion in each specimen was analyzed. Serial tissue sections (3 μm) were cut and mounted on glass slides for hematoxylin and eosin (H&E) staining, Ziehl-Neelsen (ZN) staining (Kinyoun modification [12] with Löffler's methylene blue staining), immunohistochemistry (IHC), and real-time PCR. For analysis, sections stained by H&E or IHC were scanned by Mirax Midi (Carl Zeiss, Jena, Germany), and examined using Panoramic Viewer software (3DHistech, Budapest, Hungary). Sections stained by ZN were examined under a light microscope (BX40: Olympus, Tokyo, Japan). The mycobacteria culture test results were obtained from the clinical records. The study was approved by the ethics committees of the Japan Red Cross Medical Center (approval number 381) and the Tokyo Medical and Dental University (approval number 1266). The specimens were classified according to the following factors: result of real-time PCR for *M. tuberculosis*; presence of acid-fast bacilli on ZN staining; calcification of at least 1% of a necrotic area.

Real-time PCR

The largest lesions in each section were cut out manually on glass slides and placed into autoclaved test tubes. DNA extraction was performed using standard methods [13] that were slightly modified. In brief, tissue was deparaffinized and incubated with 200 μl proteinase K solution (50 mM Tris-HCl, pH 8.0, 1 mM EDTA, 0.5% Tween 20, 100 μg/ml proteinase K) at 56°C overnight. Tris buffer (200 μl, 50 mM, pH 8.0) was added and the solution heated at 85°C for 10 min. The solution was used as template. Real-time PCR quantification of *M. tuberculosis* was performed as described elsewhere [14]. Primers and probes were designed to amplify the insertion sequence 6110 [15]. Real-time PCR was performed using the ABI PRIZM 7900HT Sequence Detection System (Applied Biosystems, Carlsbad, CA) [16] with internal standard samples of serially diluted bacterial DNA. Assays were performed three times for each sample and the mean numbers of genomes were calculated. Samples with *M. tuberculosis* detected at least twice by PCR amplification were considered positive.

Histologic evaluation

The degree of neutrophil infiltration was quantified by the maximum number of neutrophils in a 500-μm square in each lesion. The degree of lymphocytic infiltration was quantified by the mean number of lymphocytes in three 500-μm squares located at regular intervals along the fibrotic rim and including the area of the most intense lymphocytic infiltration of each lesion. Thickness of the epithelioid cell layer was estimated based on measurements at three points located at regular intervals along the border of the necrotic area and including the thickest point of each lesion. The numbers of multinucleated giant cells were also counted. Lesion size was measured by summing the sizes of the epithelioid cell layer and necrotic area.

Production of monoclonal antibody

The anti-LAM mAb was produced according to the standard protocol [17] with modification [18]. In brief, lysates of *M. tuberculosis* (ATCC25177) were fractionated on a Bio Logic DuoFlow 10 system by anion-exchange chromatography (UNO Q1 column; Bio-Rad, Hercules, CA) with a stepwise elution (based on conductivity, from 0 to 45 ms/cm in 10 equal steps and high salt wash, pH 7.0). Each fraction was injected into BALB/c mice (CLEA Japan, Tokyo, Japan) with complete Freund's adjuvant. Hybridoma cell lines producing anti-*M.*

tuberculosis antibody were examined by ELISA [16] using whole-cell lysate of *M. tuberculosis* and by IHC on FFPE tissue sections of an *M. tuberculosis*-injected rat liver (female Sprague-Dawley rats; CLEA Japan) [18] and a tubercle from human lung tissue. A hybridoma cell line generated from the mice injected with the tenth fraction was then cloned by limited dilution. A single hybridoma was implanted into the intraperitoneal space of the mice with severe combined immunodeficiency (SCID). Two weeks after implantation, ascites were collected and used as undiluted antibody. The undiluted antibody reacted with purified tuberculous LAM (Nacalai Tesque, Kyoto, Japan) in Western Blot (antibody 1:1000, LAM 20 μg per lane, Figure 1A) [16].

Immunohistochemistry

After deparaffinization, sections were microwaved (Microwave Processor H2850; Energy Beam Sciences, East Granby, CT) in 10 mM citrate buffer (pH 6.0) for 40 min at 97°C. Sections were treated with 3% hydrogen peroxide in methanol for 10 min and incubated with normal horse serum (Vectastain Universal Elite ABC Kit; Vector Laboratories, Burlingame, CA). Sections were incubated overnight with anti-LAM mAb (1:2000) or anti-BCG polyclonal antibody (pAb) (1:10000; Dako, Glostrup, Denmark) at room temperature, and for 30 min with secondary antibody (Vectastain Universal Elite ABC Kit), followed by 30-min incubation with streptavidin–peroxidase complex (Vectastain Universal Elite ABC Kit), both at room temperature. The signal was developed as a brown reaction product using DAB peroxidase substrate (Histofine Simplestain DAB Solution; Nichirei
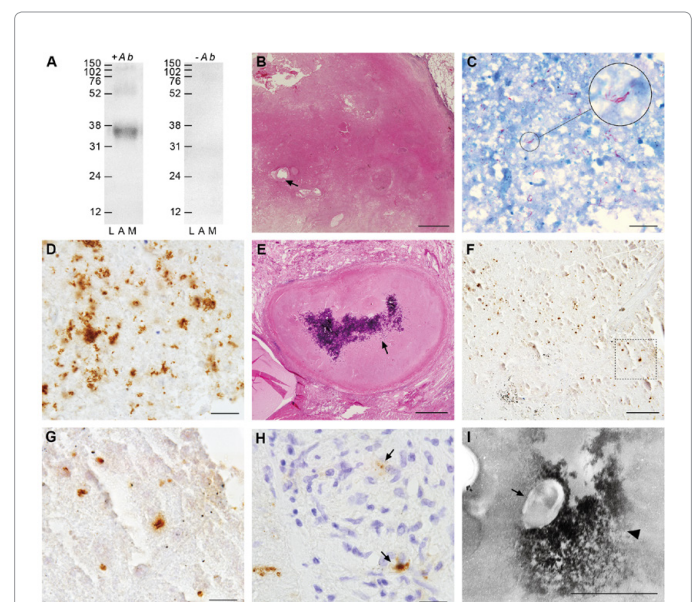

Figure 1: Calcified granulomatous lesions contained granules reacted by anti-LAM mAb in necrotic areas.

(A) Western blot analysis with novel mAb using purified LAM (left lane). Negative control with the primary antibody omitted (right lane). (B) Representative picture of a lesion in the ZN(+) group. (C) Area pointed to by the arrow in (B) with ZN staining. Inset shows acid-fast bacilli in higher magnification. (D) IHC with anti-LAM mAb in the area adjacent to (C). (E) Representative picture of a lesion from the calcification(+) group. (F) IHC with anti-LAM mAb in the area pointed to by the arrow in (E). Granular-positive reaction products were detected. (G) High magnification of the area indicated by the dashed square in (F). (H) IHC with anti-LAM mAb in a ZN(+) granuloma. A few granular positive reaction products were observed within the epithelioid cell layer (arrow). (I) Immunoelectron microscopy with anti-LAM mAb in a lesion from the calcification(+) group. DAB deposition (arrow) was observed around the bacillus-like structure (arrowhead). Scale bar= 500μm in (B)(E), 10 μm in (C)(D)(G)(H), 50 μm in (F), 1 μm in (I).

Bioscience, Tokyo, Japan). The sections were then counterstained with Mayer's hematoxylin.

Immunoelectron microscopy

FFPE tissue sections of calcified granulomatous lesions were used for immunoelectron microscopy with anti-LAM mAb [19]. In brief, paraffin sections (6-mm thick) were processed in the same manner as IHC until the secondary antibody reaction. Subsequently, the sections were fixed with 2% glutaraldehyde for 5 min and incubated with peroxidase substrate (Histofine Simplestain DAB Solution). Sections were then post-fixed with 0.5% OsO_4 for 60 min and embedded in Epon. Ultrathin sections were cut on a Reichert Ultracut S (Leica, Mannheim, Germany), collected on Maxtaform grids (Pyser-SGL, Kent, UK), and examined using an H-7100 electron microscope (Hitachi, Tokyo, Japan).

Statistical analyses

Statistical differences in the results of the histologic evaluation, real-time PCR, and count analysis of IHC among the groups were tested by the Steel-Dwass test [19,20]. The results are shown by boxplots (minimum, lower quartile, median, upper quartile and maximum). Differences with P values less than 0.05 were considered significant. The statistical software used was Statview 5.0 for Windows (SAS Institute, Cary, NC) and Excel 2007 (Microsoft, Redmond, WA).

Results

All of the calcified granulomatous lesions contained *M. tuberculosis* genomes

Of 70 granulomatous lesions with caseous necrosis, 34 (49%) were positive *M. tuberculosis* by real-time PCR. Among these 34, 24 lesions were negative by ZN staining but positive by real-time PCR. Calcification in necrotic areas, a well-known characteristic of old tuberculous lesions [3], was observed only in the ZN-negative but real-time PCR-positive lesions; no calcification was observed in the real-time PCR-negative lesions.

When comparing the sensitivity of the ZN staining with the real-time PCR method with calculation we find that: with lesions with calcification, the sensitivity is 0% (0 out of 11). While with lesions without calcification, the sensitivity is 43% (10 out of 23). Overall the sensitivity of the ZN staining is 29% (10 out of 34).

To characterize the calcified granulomatous lesions, we classified the real-time PCR-positive lesions into three groups (Figure 2); ZN (+), calcification (-), and calcification (+)] and compared the results of the culture test, the number of bacterial genomes, degrees of histologic inflammation, and lesion size among them. None of the calcification (+) lesions was positive by the culture test (Table 1). Calcification (+) lesions contained significantly more bacterial genomes than calcification (-) lesions, although ZN (+) lesions contained the most (Figure 3A). Calcification (+) lesions were small and had minimum inflammation with the thinnest epithelioid cell layer, indicating that they were the most quiescent lesions (Figure 3B-F).

Bacterial cell wall components were observed in necrotic and calcified areas

To localize *M. tuberculosis* that could not be detected by ZN staining, we generated a novel mAb against LAM (Figure 1A) and performed IHC using this mAb on the lesions (Figure 1B-1H). Positive reaction products appeared granular in a part of the necrotic area in all lesions of the ZN (+) group, all lesions of the calcification (+) group,
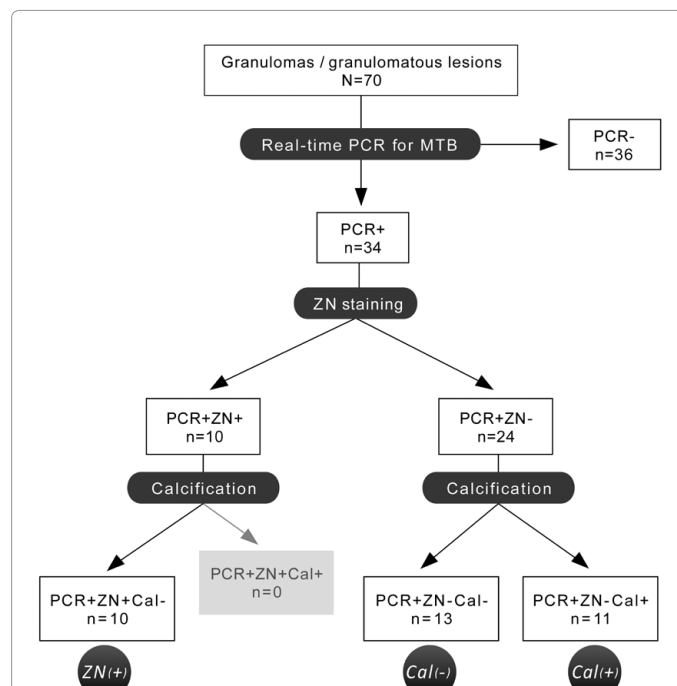

Figure 2: Calcifications were observed in the lesions positive by real-time PCR for *M. tuberculosis* and negative by ZN staining.

Seventy granulomatous lesions were screened by real-time PCR for *M. tuberculosis*. Real-time PCR-positive lesions were then checked for acid-fast bacilli by ZN staining and for the presence of calcification in necrotic areas. The lesions were classified into three groups: ZN(+), Calcification (Cal)(-) (Cal(-)), Cal(+), and PCR(-) groups.

	ZN(+) group (n=10)	Cal(-) group (n=13)	Cal(+) group (n=11)
Positive (%)[a]	4 (40)	4 (31)	0 (0)
Negative (%)[a]	4 (40)	4 (31)	10 (91)
Not performed (%)	2 (20)	5 (38)	1 (9)

[a]Results of culture for mycobacteria from surgically resected tissues.

Table 1: Results of culture test of the ZN(+), Calcification(-), and Calcification(+) groups.

and 11 of 13 lesions of the calcification (-) group. In the calcification (+) group, positive reaction products were observed in both calcified and non-calcified necrotic areas. In some lesions of the ZN (+) and calcification (-) groups, a few positive reaction products were observed in the epithelioid cell layer in addition to the necrotic area. We also performed IHC with anti-BCG pAb on the same lesions. The staining patterns of the anti-BCG pAb were almost identical with those of anti-LAM mAb (Figure 4).

Next, we counted the number of granules that reacted with the anti-LAM mAb to evaluate the correlation with the number of bacterial genomes. There tended to be correlations between them in each group, although the distributions of the data were heterogeneous (Figure 5A). Calcified granulomatous lesions contained as many granules as ZN-positive lesions, and showed the highest ratio of the number of granules divided by the number of bacterial genomes (Figure 5B and 5C).

To confirm that the granules reacted with the anti-LAM mAb indicated the locations of *M. tuberculosis*, we performed immunoelectron microscopy using the anti-LAM mAb on the calcification (+) lesions. We found bacillus-like structures surrounded
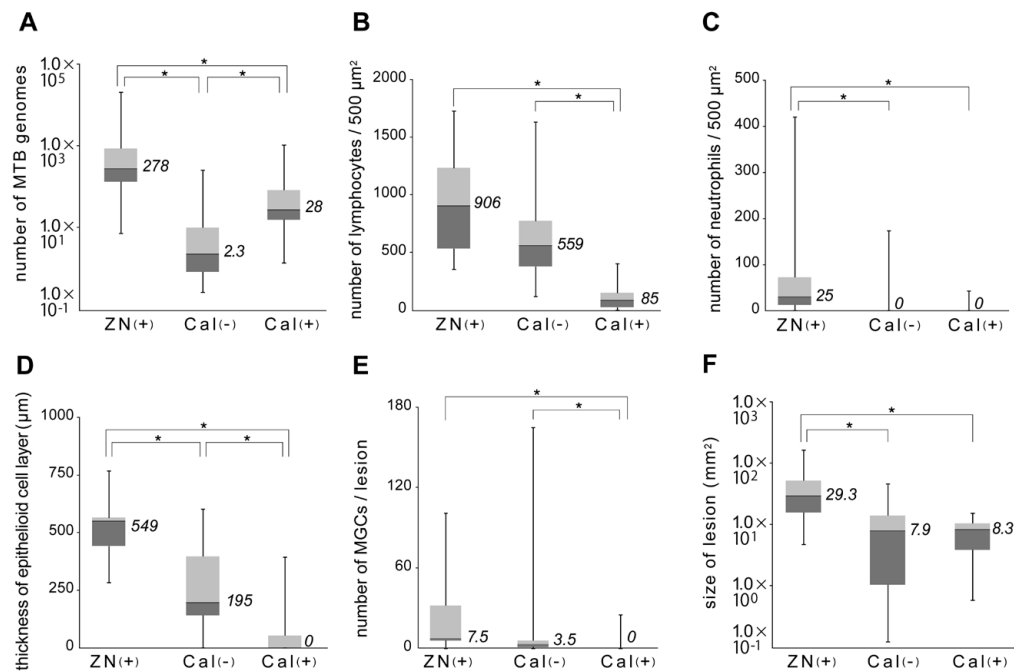
Figure 3: Calcified granulomatous lesions exhibited minimum inflammation but contained a considerable amount of bacterial genomes.

(A) Real-time PCR quantifications for *M. tuberculosis* were expressed by boxplots with logarithmic scale. (B-F) Histologic quantification of inflammation in granulomas based on the measurements of the mean numbers of lymphocytes (B), neutrophils (C), mean thickness of the epithelioid cell layer (D), and the number of multinucleated giant cells (E) in each lesion of the three groups. Results are expressed by boxplots. (F) Sizes of granulomas are expressed by boxplots with a logarithmic scale. n=10 in the ZN(+), 13 in the Cal(-), 11 in the Cal(+). * P<0.05, Steel-Dwass test.
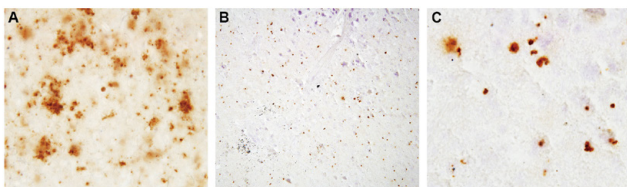

Figure 4: IHC with anti-BCG pAb showed granular positive reaction products in necrotic areas, which were similar to IHC with anti-LAM mAb.

(A-C) IHC with anti-BCG pAb. (A), (B) and (C) are the same area of adjacent sections in (D), (F) and (G) in Figure 3, respectively.

by the deposition of DAB reaction products, which seemed to discharge from the structures (Figure 1), and particles or irregularly shaped structures were also surrounded by such deposits.

Discussion

To clarify the amount and location of *M. tuberculosis* in old tuberculous lesions, which are considered hotbeds for post-primary tuberculosis and yet are negative for the conventional tests for mycobacteria, we quantified the bacterial genomes and localized bacterial cell wall components in these lesions. Our findings indicated that old granulomatous lesions of lungs, particularly lesions with calcification, contained abundant *M. tuberculosis* components in necrotic areas. All of the calcified granulomatous lesions examined were positive for *M. tuberculosis* by real-time PCR and positive by IHC against LAM in necrotic areas, although they were ZN-negative and culture-negative, and had minimum inflammation. Based on the fact that these results were obtained from thin sections of fixed tissue of

lesions, it is likely that whole lesions contained considerable amounts of bacterial components.

It is unknown whether the old lesions that were negative by culture contained viable *M. tuberculosis* and therefore carried a risk of reactivation. We believe the calcified granulomatous lesions had a risk of reactivation for the following reasons: (1) In autopsy studies of miliary tuberculosis, calcified granulomatous lesions were frequently found in the lungs, indicating their association with reactivation [21]; (2) Several studies report that *M. tuberculosis* assumes a temporarily nonculturable state *in vitro* and *in vivo* [22,23]; and (3) Our findings indicated that calcified granulomatous lesions contained many *M. tuberculosis* genomes and granules with mycobacterial cell wall components, some of which had a bacillus shape. More direct evidence, such as isolation and culture of bacteria from calcified granulomatous lesions, is needed for further confirmation.

In the IHC with anti-LAM mAb, granular positive reaction products were observed extracellularly in necrotic areas and intracellularly in the epithelioid cell layer. This staining pattern was almost identical to that of anti-BCG pAb [24,25]. IHC against some other components of *M. tuberculosis*, however, showed different staining patterns in previous studies, such as IHC with anti-MPT64 and anti-38-kDa antigen antibodies, which showed diffuse cytoplasmic staining of epithelioid cells and multinucleated giant cells [26,27]. This difference in the staining patterns may be due to anti-LAM and anti-BCG antibodies reacting with the cell wall components of *M. tuberculosis* whereas anti-MPT64 and anti-38-kDa antigen antibodies react with the secreted or free proteins from *M. tuberculosis*.

Calcified granulomatous lesions contained many granules that reacted with the anti-LAM mAb, relative to the number of bacterial genomes. This finding suggests that the lesions contained
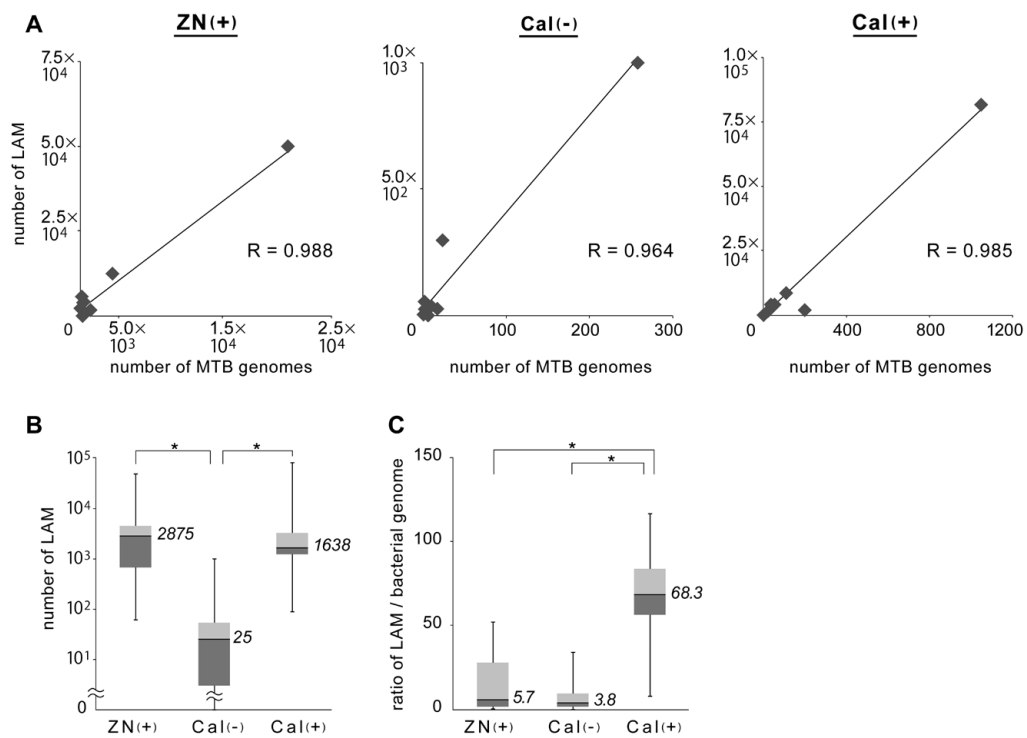
Figure 5: Calcified granulomatous lesions contained many granules reacted by anti-LAM mAb relative to the number of bacterial genomes.

(A) Correlation graphs of the number of LAM-containing granules and the number of bacterial genomes in the three groups. Correlation coefficient=0.988 in ZN(+) group, 0.964 in Cal(-) group, and 0.985 in Cal(+) group. (B) Numbers of LAM-containing granules in the three groups are expressed by boxplots on a logarithmic scale. (C) Ratios of the number of LAM containing granules divided by the number of bacterial genomes in the three groups are expressed by boxplots. n=10 in the ZN(+), 13 in the Cal(-), 11 in the Cal(+). *P<0.05, Steel-Dwass test.

abundant bacterial debris or cell wall components without genomes. Immunoelectron microscopy revealed that substances that reacted with anti-LAM mAb seemed to discharge from the bacillus-like structures to the surrounding necrotic tissue. These substances would remain after the disappearance of the bacteria due to transfer or death.

ZN staining should be an insufficient method for detecting tubercle bacilli in old tubercles, particularly with calcification. Based on the results by the real-time PCR for *M. tuberculosis*, overall the sensitivity of the ZN staining was 29% (10 out of 34), and with lesions with calcification the sensitivity was 0% (0 out of 11). These are in fact very low sensitivity, indicating that most samples drown from old lesions for diagnosis with ZN staining usually comes negative. In contrast, IHC with anti-LAM mAb showed a high sensitivity that overall the sensitivity was 94% (32 out of 34) and with lesions with calcification the sensitivity was 100% (11 out of 11). PCR for bacterial genomes and IHC with monoclonal antibodies remain the best methods for detection and identification of tubercle bacilli as well as other forms of infectious microorganisms.

We showed that old foci of tuberculosis, particularly those exhibiting some calcification, contained abundant *M. tuberculosis* components in necrotic areas. The presence of calcified lesions in the lungs, therefore, appears to be a hallmark of an M. tuberculosis carrier, which could be detected by imaging tests clinically. The risk of reactivation of latent tuberculosis from these calcified lesions should be considered, especially in patients who have a high risk of secondary tuberculosis, such as acquired immune deficiency syndrome, diabetic mellitus, and other immunosuppressed patients.

References

1. Dye C, Glaziou P, Floyd K, Raviglione M (2013) Prospects for tuberculosis elimination. Annu Rev Public Health 34: 271-286.

2. Mack U, Migliori GB, Sester M, Rieder HL, Ehlers S, et al. (2009) LTBI: latent tuberculosis infection or lasting immune responses to M. tuberculosis? A TBNET consensus statement. Eur Respir J 33: 956-973.

3. Corrin B, Nicholson AG (2011) Pathology of the Lungs. (3rd edn), Churchill Livingstone, Edinburgh.

4. Gupta A, Kaul A, Tsolaki AG, Kishore U, Bhakta S (2012) Mycobacterium tuberculosis: immune evasion, latency and reactivation. Immunobiology 217: 363-374.

5. Tang YW, Procop GW, Zheng X, Myers JL, Roberts GD (1998) Histologic parameters predictive of mycobacterial infection. Am J Clin Pathol 109: 331-334.

6. Cardona PJ (2010) Revisiting the natural history of tuberculosis. The inclusion of constant reinfection, host tolerance, and damage-response frameworks leads to a better understanding of latent infection and its evolution towards active disease. Arch Immunol Ther Exp (Warsz) 58: 7-14.

7. Kapoor N, Pawar S, Sirakova TD, Deb C, Warren WL, et al. (2013) Human granuloma in vitro model, for TB dormancy and resuscitation. PLoS One 8: e53657.

8. Deb C, Lee CM, Dubey VS, Daniel J, Abomoelak B, et al. (2009) A novel in vitro multiple-stress dormancy model for Mycobacterium tuberculosis generates a lipid-loaded, drug-tolerant, dormant pathogen. PLoS One 4: e6077.

9. Bhatt A, Fujiwara N, Bhatt K, Gurcha SS, Kremer L, et al. (2007) Deletion of kasB in Mycobacterium tuberculosis causes loss of acid-fastness and subclinical latent tuberculosis in immunocompetent mice. Proc Natl Acad Sci U S A 104: 5157-5162.

10. Gómez-Laguna J, Carrasco L, Ramis G, Quereda JJ, Gómez S, et al. (2010) Use of real-time and classic polymerase chain reaction assays for the diagnosis of porcine tuberculosis in formalin-fixed, paraffin-embedded tissues. J Vet Diagn Invest 22: 123-127.

11. Mishra AK, Driessen NN, Appelmelk BJ, Besra GS (2011) Lipoarabinomannan and related glycoconjugates: structure, biogenesis and role in Mycobacterium tuberculosis physiology and host-pathogen interaction. FEMS Microbiol Rev 35: 1126-1157.

12. Chaplin KC, Lauderdale TL (2007) Reagents, stains, and media: bacteriology: Manual of Clinical Microbiology. (9th edn), ASM Press, Washington, D.C.

13. Sato Y, Sugie R, Tsuchiya B, Kameya T, Natori M, et al. (2001) Comparison of the DNA extraction methods for polymerase chain reaction amplification from formalin-fixed and paraffin-embedded tissues. Diagn Mol Pathol 10: 265-271.

14. Eishi Y, Suga M, Ishige I, Kobayashi D, Yamada T, et al. (2002) Quantitative analysis of mycobacterial and propionibacterial DNA in lymph nodes of Japanese and European patients with sarcoidosis. J Clin Microbiol 40: 198-204.

15. Fidler H, Rook GA, Johnson NM, McFadden JJ (1993) Specificity of primers based on IS6110 to Mycobacterium tuberculosis complex DNA. Tuber Lung Dis 74: 414-415.

16. Ito T, Kobayashi D, Uchida K, Takemura T, Nagaoka S, et al. (2008) Helicobacter pylori invades the gastric mucosa and translocates to the gastric lymph nodes. Lab Invest 88: 664-681.

17. Hikawa N, Takenaka T (1997) Method for production of neuronal hybridoma using emetine and actinomycin D. Brain Res Brain Res Protoc 1: 224-226.

18. Negi M, Takemura T, Guzman J, Uchida K, Furukawa A, et al. (2012) Localization of propionibacterium acnes in granulomas supports a possible etiologic link between sarcoidosis and the bacterium. Mod Pathol 25: 1284-1297.

19. Steel RGD (1960) A Rank Sum Test for Comparing All Pairs of Treatments. Technometrics 2: 197-207.

20. Dwass M (1960) Some k-sample rank-order tests: Contributions to Probability and Statistics, Stanford University Press, Stanford.

21. Tajiri T, Tate G, Makino M, Akita H, Omatsu M, et al. (2011) Autopsy cases of military tuberculosis: clinicopathologic features including background factors. J Nippon Med Sch 78: 305-311.

22. Subbian S, Tsenova L, O'Brien P, Yang G, Kushner NL, et al. (2012) Spontaneous latency in a rabbit model of pulmonary tuberculosis. Am J Pathol 181: 1711-1724.

23. Shleeva MO, Kudykina YK, Vostroknutova GN, Suzina NE, Mulyukin AL, et al. (2011) Dormant ovoid cells of Mycobacterium tuberculosis are formed in response to gradual external acidification. Tuberculosis (Edinb) 91: 146-154.

24. Ulrichs T, Lefmann M, Reich M, Morawietz L, Roth A, et al. (2005) Modified immunohistological staining allows detection of Ziehl-Neelsen-negative Mycobacterium tuberculosis organisms and their precise localization in human tissue. J Pathol 205: 633-640.

25. Seiler P, Ulrichs T, Bandermann S, Pradl L, Jörg S, et al. (2003) Cell-wall alterations as an attribute of Mycobacterium tuberculosis in latent infection. J Infect Dis 188: 1326-1331.

26. Ihama Y, Hokama A, Hibiya K, Kishimoto K, Nakamoto M, et al. (2012) Diagnosis of intestinal tuberculosis using a monoclonal antibody to Mycobacterium tuberculosis. World J Gastroenterol 18: 6974-6980.

27. Mustafa T, Wiker HG, Mfinanga SG, Morkve O, Sviland L (2006) Immunohistochemistry using a Mycobacterium tuberculosis complex specific antibody for improved diagnosis of tuberculous lymphadenitis. Mod Pathol 19: 1606-1614.